

Towards the design of efficient quantum dot light-emitting diodes by controlling the exciton lifetime

Wenyu Ji,¹ Qinghui Zeng,¹ Pengtao Jing,^{1,3} Ming-Ming Jiang,¹ Songnan Qu,¹ Di Li,¹ Jia Wang,^{1,2} and Chong-Xin Shan^{1,*}

¹State Key Laboratory of Luminescence and Applications, Changchun Institute of Optics, Fine Mechanics and Physics, Chinese Academy of Sciences, Changchun 130033, China

²Department of Physics, Jilin University, Changchun 130012, China

³jingpt@ciomp.ac.cn

*shancx@ciomp.ac.cn

Abstract: Time-resolved photoluminescence and electroluminescence measurements were used to explore the emission characteristics of excitons in quantum dot light-emitting diodes (QD-LEDs). It is found that the lifetime of excitons in the QDs can be varied by adjusting the distance between the excitons and metal Al mirror, which is due to the effect of local density of optical states (LDOS) on the exciton decay rate. QD-LEDs with different hole transport layer (HTL) thickness, i.e., different distance between QDs and Al reflective anode, have been fabricated and it is found that the HTL thickness affects the device efficiency performance greatly, and the optimal HTL thickness for the red QD-LED (emission peak is at 621 nm) is 80 nm. These results shed light on the factors affecting the efficiency and efficiency roll-off in QD-LEDs, thus may provide a clue for high performance QD-LEDs.

©2015 Optical Society of America

OCIS codes: (230.3670) Light-emitting diodes; (230.5590) Quantum-well, -wire and -dot devices; (160.2540) Fluorescent and luminescent materials; (310.6845) Thin film devices and applications.

References and links

1. V. L. Colvin, M. C. Schlamp, and A. P. Alivisatos, "Light-emitting-diodes made from cadmium selenide nanocrystals and a semiconducting polymer," *Nature* **370**(6488), 354–357 (1994).
2. H. Shen, S. Wang, H. Wang, J. Niu, L. Qian, Y. Yang, A. Titov, J. Hyvonen, Y. Zheng, and L. S. Li, "Highly efficient blue-green quantum dot light-emitting diodes using stable low-cadmium quaternary-alloy ZnCdSSe/ZnS core/shell nanocrystals," *ACS Appl. Mater. Interfaces* **5**(10), 4260–4265 (2013).
3. Y. Zhang, C. Xie, H. Su, J. Liu, S. Pickering, Y. Wang, W. W. Yu, J. Wang, Y. Wang, J. I. Hahm, N. Dellas, S. E. Mohney, and J. Xu, "Employing heavy metal-free colloidal quantum dots in solution-processed white light-emitting diodes," *Nano Lett.* **11**(2), 329–332 (2011).
4. B. K. Chen, H. Z. Zhong, W. Q. Zhang, Z. A. Tan, Y. F. Li, C. R. Yu, T. Y. Zhai, Y. Bando, S. Y. Yang, and B. S. Zou, "Highly emissive and color-tunable CuInS₂-based colloidal semiconductor nanocrystals: off-stoichiometry effects and improved electroluminescence performance," *Adv. Funct. Mater.* **22**(10), 2081–2088 (2012).
5. V. Wood and V. Bulović, "Colloidal quantum dot light-emitting devices," *Nano Rev.* **1**(0), 5202 (2010).
6. Y. Shirasaki, G. J. Supran, M. G. Bawendi, and V. Bulović, "Emergence of colloidal quantum-dot light-emitting technologies," *Nat. Photonics* **7**(1), 13–23 (2012).
7. T.-H. Kim, K.-S. Cho, E. K. Lee, S. J. Lee, J. Chae, J. W. Jung, W. Kim, D. H. Kim, J.-Y. Kwon, G. Amaratunga, S. Y. Lee, B. L. Choi, Y. Kuk, J. M. Kim, and K. Kim, "Full-colour quantum dot displays fabricated by transfer printing," *Nat. Photonics* **5**(3), 176–182 (2011).
8. K. S. Cho, E. K. Lee, W.-J. Joo, E. Jang, T.-H. Kim, S. J. Lee, S.-J. Kwon, J. Y. Han, B.-K. Kim, B. L. Choi, and J. M. Kim, "High-performance crosslinked colloidal quantum-dot light-emitting diodes," *Nat. Photonics* **3**(6), 341–345 (2009).
9. J. Kwak, W. K. Bae, D. Lee, I. Park, J. Lim, M. Park, H. Cho, H. Woo, Y. Yoon, K. Char, S. Lee, and C. Lee, "Bright and efficient full-color colloidal quantum dot light-emitting diodes using an inverted device structure," *Nano Lett.* **12**(5), 2362–2366 (2012).

10. B. S. Mashford, M. Stevenson, Z. Popovic, C. Hamilton, Z. Zhou, C. Breen, J. Steckel, V. Bulović, M. Bawendi, S. Coe-Sullivan, and P. T. Kazlas, "High-efficiency quantum-dot light-emitting devices with enhanced charge injection," *Nat. Photonics* **7**(5), 407–412 (2013).
11. W. Ji, P. Jing, J. Zhao, X. Liu, A. Wang, and H. Li, "Inverted CdSe/CdS/ZnS quantum dot light emitting devices with titanium dioxide as an electron-injection contact," *Nanoscale* **5**(8), 3474–3480 (2013).
12. X. Dai, Z. Zhang, Y. Jin, Y. Niu, H. Cao, X. Liang, L. Chen, J. Wang, and X. Peng, "Solution-processed, high-performance light-emitting diodes based on quantum dots," *Nature* **515**(7525), 96–99 (2014).
13. E. Matioli, S. Brinkley, K. Kelchner, Y. Hu, S. Nakamura, S. DenBaars, J. Speck, and C. Weisbuch, "High-brightness polarized light-emitting diodes," *Light Sci. Appl.* **1**(8), e22 (2012).
14. C. Xiang, W. Koo, F. So, H. Sasabe, and J. Kido, "A systematic study on efficiency enhancements in phosphorescent green, red and blue microcavity organic light emitting devices," *Light Sci. Appl.* **2**(6), e74 (2013).
15. W. Y. Ji, P. T. Jing, and J. L. Zhao, "Improving the efficiency and reducing efficiency roll-off in quantum dot light emitting devices by utilizing plasmonic Au nanoparticles," *J. Mater. Chem. C Mater. Opt. Electron. Devices* **1**(3), 470–476 (2013).
16. W. K. Bae, Y.-S. Park, J. Lim, D. Lee, L. A. Padilha, H. McDaniel, I. Robel, C. Lee, J. M. Pietryga, and V. I. Klimov, "Controlling the influence of Auger recombination on the performance of quantum-dot light-emitting diodes," *Nat. Commun.* **4**, 2661 (2013).
17. T. Tsutsui, C. Adachi, S. Saito, M. Watanabe, and M. Koishi, "Effect of confined radiation-field on spontaneous-emission lifetime in vacuum-deposited fluorescent dye films," *Chem. Phys. Lett.* **182**(2), 143–146 (1991).
18. R. R. Chance, A. Prock, and R. Silbey, "Lifetime of an excited molecule near a metal mirror: Energy transfer in the Eu^{3+} silver system," *J. Chem. Phys.* **60**(5), 2184–2185 (1974).
19. H. Becker, S. E. Burns, and R. H. Friend, "Effect of metal films on the photoluminescence and electroluminescence of conjugated polymers," *Phys. Rev. B* **56**(4), 1893–1905 (1997).
20. W. Ji, P. Jing, L. Zhang, D. Li, Q. Zeng, S. Qu, and J. Zhao, "The work mechanism and sub-bandgap-voltage electroluminescence in inverted quantum dot light-emitting diodes," *Sci. Rep.* **4**, 6974 (2014).
21. W. Ji, Y. Tian, Q. Zeng, S. Qu, L. Zhang, P. Jing, J. Wang, and J. Zhao, "Efficient quantum dot light-emitting diodes by controlling the carrier accumulation and exciton formation," *ACS Appl. Mater. Interfaces* **6**(16), 14001–14007 (2014).
22. W. Ji, L. Zhang, R. Gao, L. Zhang, W. Xie, H. Zhang, and B. Li, "Top-emitting white organic light-emitting devices with down-conversion phosphors: Theory and experiment," *Opt. Express* **16**(20), 15489–15494 (2008).
23. H. Sung, J. Lee, K. Han, J. Lee, J. Sung, D. Kim, M. Choi, and C. Kim, "Controlled positioning of metal nanoparticles in an organic light-emitting device for enhanced quantum efficiency," *Org. Electron.* **15**(2), 491–499 (2014).

1. Introduction

Colloidal quantum dots (QDs) have attracted tremendous attention in the past decades for their fascinating properties, such as high emission efficiency, narrow emission spectrum, tunable emission from ultraviolet (UV) to near infrared, and facile processibility via low-cost solution-based techniques, and have been used in many applications [1–6]. Particularly, QDs based light-emitting diodes (QD-LEDs), which possess reduced power consumption and compatibility with flexible substrates, have been considered as promising candidate for next-generation flat panel displays and lighting sources [5,6]. The utilization of inorganic electron transport materials such as ZnO and TiO_2 allows injecting electrons into QDs effectively, which enables further improved efficiency in QD-LEDs [7–11]. To date, the maximum external quantum efficiency is over 20% [12], exceeding that of fluorescent organic LEDs that have been extensively investigated for over two decades [13,14]. Although some steady progresses have been achieved, there are still some serious issues to be overcome. On one hand, the efficiency of the QD-LEDs is currently lagging behind the organic phosphorescent LEDs and there is still large room to further improve the device performance. On the other hand, efficiency roll-off, referring to the decrease in the electroluminescence (EL) efficiency at large current density or luminance, still remains a big obstacle to efficient device and is barely investigated. The efficiency roll-off in QD-LEDs predominantly originates from the exciton quenching induced by the QD charging or/and Auger recombination (AR) induced by extra charges [15,16]. In QD-LEDs, QD charging and AR processes are facilitated due to imbalanced charge injection and low radiative rate of QDs. Especially, the QD charging or AR process becomes more severe under high operation current in the QD-LEDs due to more excessive charges injected into the QDs. It has been reported that the QD charging or/and AR processes can be greatly suppressed by introducing gold nanoparticles or QD structure engineering [15,16], which reduces device efficiency roll-off and increases device efficiency dramatically due to the increased exciton radiative rate in QDs. Therefore, how to control the

exciton radiative rate of QDs in QD-LEDs becomes an urgent problem to be solved towards improved device performance.

In usual QD-LEDs, the competition between radiative and nonradiative decay processes in QDs is rather important because it governs the emission efficiency of QD-LEDs. It has been demonstrated that the confined radiation field influences the emission lifetime of a fluorescent dye located near a metallic mirror greatly [17–19]. Noting that this high reflective metal electrode in common QD-LEDs also acts as a mirror that reflects the light from the QDs, altering the distribution of the confined radiation field or local density of optical states (LDOS). In typical QD-LED architectures, the excitons are located within tens of nanometers from the high reflective electrode and the decay rate of excitons must be influenced by the nearby metallic mirror due to interactions with the reflected confined electric field [17,18]. Therefore, the distance between excitons and reflective metal electrode plays a rather crucial role in QD-LED performance. However, none report on the effect of the LDOS on QD-LED performance can be found to date.

In this study, we have highlighted, for the first time, the effect of LDOS on the performance of QD-LEDs. Here we selected the inverted QD-LED structure because its work mechanism only relies on direct injection of charges into QDs from adjacent charge transport layer [10,20], which allows us to correlate the spectroscopic results with the overall device performance in the regime of electrical injection more easily. The LDOS is controlled by adjusting the thickness of hole transport layer (HTL) in the inverted QD-LEDs. Time-resolved photoluminescence (TRPL) measurements were used to study changes in the lifetime of excitons located at different distances (from 20 nm to 150 nm) away from the metallic mirror.

2. Experimental details

For the PL measurements, the samples with a structure of Glass/ZnO (40 nm)/QDs (25 nm)/4,4'-N,N'-dicarbazole-biphenyl (CBP, 10 nm)/CBP:MoO₃ (15%, y nm)/Al (100 nm) were prepared with y varying from 10 to 140. The distance (d) between QDs/CBP interface and Al film is varied from 20 to 150 nm. Two samples (R1 and R2) with the same structure ($y = 10$) in the absence of Al film were also built, where 10 and 100 nm CBP layers were adopted for R1 and R2, respectively. Both the TRPL and steady-state PL measurements were carried out with an Edinburgh Instruments FL920 spectrometer utilizing a 485 nm excitation light source that can excite the QDs only. The reflectance spectrum was measured with an ultraviolet/visible spectrometer (UV 1700, Shimadzu). The refractive indices (measured with a variable angle spectroscopic ellipsometry) of ZnO nanoparticles, QDs, and CBP at 610 nm is 1.70, 1.64, and 1.65, respectively. The relatively low refractive index of the QD thin film is mainly due to the organic ligands and interspace between QDs.

In order to demonstrate the effect of LDOS on the device performance, a set of QD-LEDs with a structure of glass coated ITO/ZnO (40 nm)/QDs (25 nm)/CBP (45 nm)/CBP:MoO₃ (15%, x nm)/Al (100 nm) were fabricated. The value of x is varied from 5 nm to 45 nm for different devices, A (5 nm, $d = 50$ nm), B (15 nm, $d = 60$ nm), C (25 nm, $d = 70$ nm), D (35 nm, $d = 80$ nm), and E (45 nm, $d = 90$ nm), the corresponding distance between the QD emitters and high reflective Al anode is varied from 50 to 90 nm due to the excitons being formed at QDs/CBP interface as reported previously [20,21]. Before use, the ITO substrates were ultrasonically cleaned with a standard process as described in our previous report [21], and underwent an ex situ UV ozone treatment in air for 5 min. The ZnO and QD films are deposited by a spincoating technique and CBP and CBP:MoO₃ films are achieved by thermal evaporation process. The detailed fabrication and measurements processes for the QD-LEDs have been described in our previous papers [20–22]. The ZnO nanoparticles and red CdSe/ZnS core-shell QDs were synthesized with a method described before [12,20].

3. Results and discussion

For the PL measurements, the samples were fabricated with the structure shown in the inset of Fig. 1(a). CBP/CBP:MoO₃ was used as a spacer to adjust the distance between the QDs and Al mirror. It is accepted that the uniformity and precise thickness control of CBP/CBP:MoO₃

layer are very crucial because variations in the refractive index and thickness of the CBP/CBP:MoO₃ layer will result in the deviations of the measured TRPL curves and affect the reproducibility of the TRPL measurements. The typical decay curves of the QDs for sample with $d = 80$ nm are shown in Fig. 1(a). One can see that the five TRPL curves taken from different area of the samples are almost identical with each other, indicating the good uniformity of the samples fabricated in our work and also demonstrating the reliability of the measurement results. Despite the good uniformity of the samples, we still recorded 5 decay curves from different areas of each sample, yielding an average of all the decay curves for each sample to obtain more convincing results. The TRPL measurements were also implemented for the two reference samples with 10 nm and 100 nm CBP layer as depicted in the Experimentals section. The exciton lifetimes for the two samples are rather identical as shown in the Fig. 1(b), which eliminates the effect of CBP:MoO₃ on the exciton decay process when a pure CBP layer (> 10 nm) is inserted.

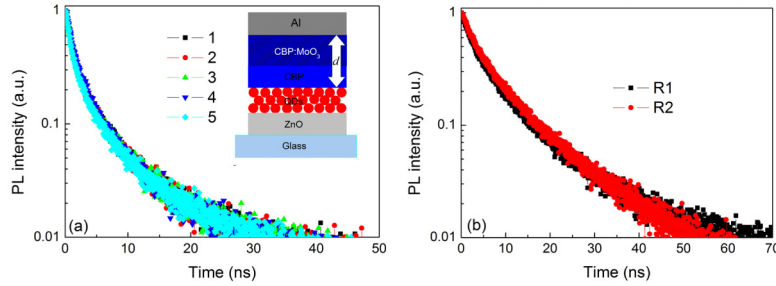


Fig. 1. (a) TRPL curves measured at different probing points for the sample with the distance of $d = 80$ nm. Inset is the schematic structure of the samples for TRPL and steady state PL measurements. (b) TRPL curves of R1 and R2.

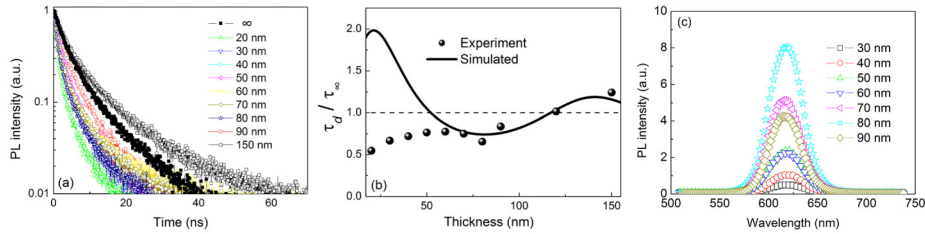


Fig. 2. (a) TRPL curves for samples with different distance between QD layer and Al mirror. (b) The normalized lifetimes of samples and the theoretical results. (c) Steady state PL spectra for the samples with distances from 30 to 90 nm.

Figure 2(a) shows the averaged curves for the 10 samples. Each decay curve is fitted with a two-exponential decay formula and the normalized lifetimes are shown in Fig. 2(b) as a function of d , where τ_d is the lifetime of emitters in the presence of Al reflective film and τ_∞ is the lifetime of excitons in the absence of the Al mirror. As can be seen from Fig. 2(b), the lifetimes exhibits a damped oscillation as the function of d since the phase and state density of the reflected field change with the distance, in line with the following theoretical prediction for a single mirror configured model [18]. The reduction of the oscillation amplitude with increasing the distance is due to the decreased radiation field of the dipole/exciton with the distance between the emitter and its mirror image. Note that the lifetime is very short (3.7-5.2 ns) when the HTL thickness is thin (less than 50 nm), which is conflict with the theoretical results. This phenomenon can be explained by the diffusion of Al atoms into the CBP or QD layer during the thermal evaporation process, which will quench the QD emission and decrease the exciton lifetime, similar to the results reported previously [23]. When the distance between the Al mirror and QDs is over 50 nm, the effect of the penetrated Al atoms on the exciton decay vanishes and the shortest lifetime of 4.4 ns is obtained when the distance

is 80 nm. Figure 2(c) shows the steady-state PL results for the samples with different spacer thicknesses. The PL intensity is enhanced with increasing the distance until to 80 nm, then it is decreases with larger spacer thickness. Considering the TRPL measurement results and the effect of Al atoms penetrated into the CBP or QD layer, these results indicate that the increased PL intensity observed for the distance over 50 nm may arise from an increased photoluminescence quantum yield of the QD layer. In general, the PL intensity I_{pl} is given by the following expression

$$I_{pl} \propto N_{Abs} \eta_{pl} = N_{Abs} \frac{k_R}{k_R + k_{NR}}.$$

Here N_{Abs} is the number of photons absorbed by the QDs, i.e., the exciton concentration. η_{pl} is the quantum yield of the QDs. k_R is the radiative decay rate and k_{NR} is the nonradiative decay rate of the excitons in the QDs. Considering that the same excitation power density and large band-gap CBP are used, N_{Abs} (or the exciton concentration) should not be changed appreciably within the QD film, indicating that differences in PL intensity cannot originate from excitation or absorption. Also, considering that a reduction in spacer thickness (from 150 nm to 80 nm) leads to a shortened PL decay lifetime, it follows, from exciton lifetime $\tau = 1/(k_R + k_{NR})$, that the decreased lifetime may originate from an increase k_{NR} if the excitons are quenched by the metal as reducing the distance. But it is not the case because the large band-gap of CBP that acts as an exciton blocking layer and prevents this quenching effect. Therefore the higher I_{pl} in the sample with the thinner CBP layer must originate from a increased k_R , meaning an increase in decay rate of excitons in the QDs, which is resulted from the interactions between excitons and the metal layer. In other words, the effect should originate from the confined radiation field reflected by the metal layer, i.e., the changes of LDOS near QDs, which is similar to the case of organic emissive dye in front of a metal mirror reported by Tsutsui and Becker [17,19].

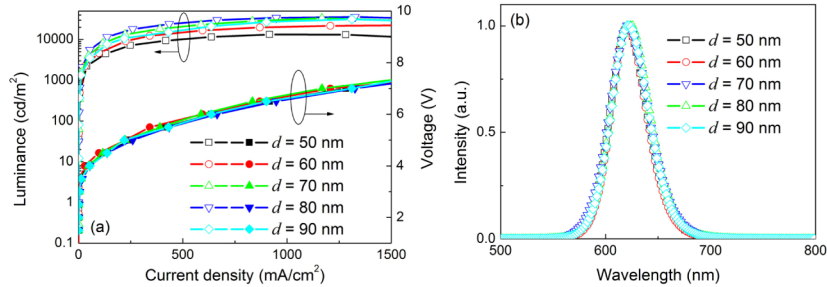


Fig. 3. (a) Luminance–voltage–current density characteristics of the QD-LEDs for different thickness (d). (b) Normalized EL spectra at operation voltage of 4.5 V for devices A ($d = 50$ nm), B ($d = 60$ nm), C ($d = 70$ nm), D ($d = 80$ nm), and E ($d = 90$ nm).

In order to verify the effect of the HTL thickness on the device performance, a series of QD-LEDs with different HTL thickness were fabricated on ITO substrates with a similar configuration as shown in the inset of Fig. 1(a). A p-doped HTL of CBP:MoO₃ is adopted in order to minimize the variations in hole transportation properties induced by the different HTL thickness among these devices. The luminance–current–voltage characteristics of the QD-LEDs are shown in Fig. 3(a). As shown in the figure, the current density for a given driving voltage varies rather modestly among the five devices, which indicates that the differences in the p-doped HTL thickness indeed have little influence on the charge transportation, suggesting they do not alter the charge balance and the location of the exciton formation zone in the emission layer significantly. Similar to the trend of PL intensity shown in Fig. 2(c), the device luminance is enhanced with increasing the HTL thickness until the distance reaches 80 nm. The maximum luminance is increased from 11,000 cd/m² for device A to 35,885 cd/m² for device D, an enhancement factor of 2.26 is achieved. Figure 3(b) shows

the EL spectra of the devices at a driving voltage of 4.5 V. As can be seen, a pure and saturated red emission (emission peak is at 621 nm) originating from the QDs is observed for all the QD-LEDs, which indicates a highly radiative recombination efficiency originating from the QD band emission and further demonstrates the p-doped HTL thicknesses have no significant influence on the location of the exciton formation zone in the QD-LEDs.

Figure 4(a) shows the current density versus efficiency curves of the five devices. As can be seen, the device efficiency is enhanced as the HTL thickness increases and the maximum current efficiency is 12.0 cd/A when a 80 nm HTL (45 nm CBP and 35nm p-doped CBP:MoO3) is used. Further increasing the HTL thickness deteriorates the device efficiency. It is noteworthy that, despite the different excitation sources to the QDs in PL and EL, the same trends are observed, as shown in Fig. 2(c) and Fig. 4(a), that is, the maximum emission efficiencies are achieved at $d = 80$ nm in both cases. This phenomenon reveals the key role of LDOS in exciton decay process. The normalized current efficiency as a function of applied current density is shown in Fig. 4(b). Note that the efficiency roll-off is reduced as increasing the HTL thickness and the smallest efficiency roll-off is obtained when the thickness of HTL is 80 nm. The decreased efficiency roll-off may be attributed to the effect of LDOS. The larger LDOS accelerates the radiative decay of the excitons, which will reduce the possibility of QD charging or/and AR at high applied current as reported previously [15].

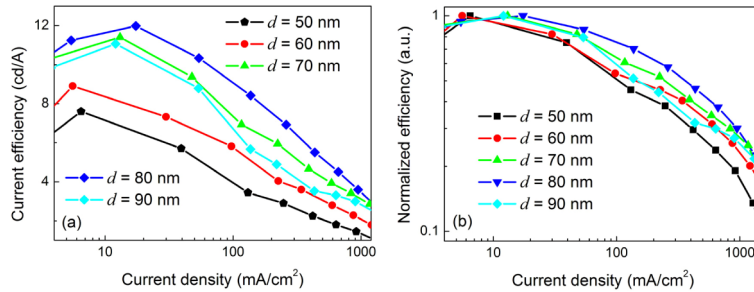


Fig. 4. (a) Current efficiency versus current density curves for the QD-LEDs, A ($d = 50$ nm), B ($d = 60$ nm), C ($d = 70$ nm), D ($d = 80$ nm), and E ($d = 90$ nm) (b) The normalized current efficiency for the QD-LEDs at different operation current density.

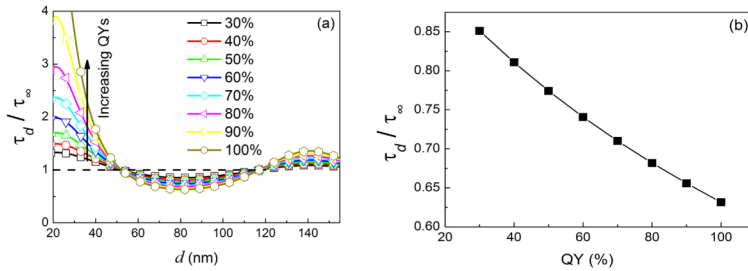


Fig. 5. The theoretical normalized lifetimes of QDs with different quantum yield as a function of distance (a) and at fixed distance of 80 nm (b).

Figure 5(a) shows the calculated normalized lifetimes of QDs with different quantum yields as a function of the HTL thickness. It is interesting that more significant impact of LDOS (or distance between QDs and Al film) on the lifetime is observed for QDs with higher quantum yield, which can be explained as follows: As discussed above, the LDOS will affect the radiative process of excitons in QDs greatly, i.e., the value of k_R . It is well known that the quantum yield can be expressed by the formula of $\eta_{pl} = k_R / (k_R + k_{NR})$. Thus, QDs with higher quantum yield must possess a larger k_R / k_{NR} value, which results in a greater effect of LDOS on the exciton lifetime in QDs, as shown in Fig. 5(b). This result reveals that the elaborate

design of the device structure is becoming more and more important as high quantum yield QDs are employed as the active layer of the QD-LEDs.

4. Conclusion

In summary, TRPL studies show that the lifetime of excitons in QDs can be modified when in close proximity to a metal mirror. Theoretical analysis also reveals the dependence of exciton lifetime on the LDOS/distance. QD-LED EL results show that with an appropriate HTL thickness, both efficiency and efficiency roll-off of the devices are improved, which is due to the increased exciton radiative rate and quantum yield of the QDs as demonstrated in spectroscopy measurements. The increased radiative rate of the excitons is in favor of suppressing the quenching processes (especially under high operation current densities) such as QD charging and AR processes. In addition, it is also demonstrated that a greater effect of LDOS on device performance will occur for QDs with higher quantum yield. Our results shed light on the factors affecting the efficiency behavior of QD-LEDs. We believe that the results reported in this paper can provide much deep insights for device design and mechanism that can help to improve the performance of QD-LEDs.

Acknowledgments

This research was supported by the National Natural Science Foundation of China (NSFC) (Nos. 61205025, 11204298, 61275197, and 61274126) and Science and Technology Development Project of Jilin Province (Nos. 20130206105SF and 20150101190JC).